Estimating and Controlling Atomic Chlorine Concentration via Actinometry

C. K. Hanish, J. W. Grizzle and **F. L. Terry, Jr.**

Abstract

Actinometry has been used as the basis of a successful sensor for controlling fluorine concentration in fluoro-carbon plasmas commonly employed in etching. An analogous sensor would be useful for chlorine plasmas as well. One problem with actinometry in Cl_2 plasmas is that excitation can occur by electron impact dissociation and by dissociative attachment, leading to potential ambiguity between the intensity of observed chlorine emission in a plasma and the actual concentration of chlorine. On the basis of a simple model, this paper analyzes the consequences of the dissociative excitation pathway on the accuracy of the estimation and control of chlorine concentration via actinometry. When the contribution of the dissociative excitation pathway is known, it is shown that asymptotic observer theory can be used to improve the accuracy of the estimation of chlorine concentration.

I. Introduction

One of the important parameters during a dry etch is the concentration of the reactive species in the plasma. When reactive gases are used in a dry etch, the etch rate is higher than the pure sputter rate [15, 21]. For example, it has been shown that in CF_4 plasmas, atomic fluorine is the key reactive species [10]. In Cl_2 plasmas, however, the reactant species is either Cl_2 or Cl, depending on the material being etched. The roles of these species for various materials are not fully understood. Molecular chlorine will not spontaneously etch N^+ polysilicon at room temperature [21] but will etch aluminum [7, 22, 23]. In contrast, Cl spontaneously etches silicon [15, 22, 23, 25] but etches Al four times more slowly than Cl_2 does [7]. It is believed that Cl_2 only adsorbs onto the top layer of Si while the chlorine atom can permeate through several layers. Ion energy assists the mixing of Si and Cl_2, however, and in this case significant etching is observed at room temperature with molecular chlorine.

In order to better understand the effects of Cl_2 and Cl on various materials, it is necessary to measure their concentrations. For materials where Cl is the main reactive species, tightly regulating the atomic chlorine concentration in the plasma should result in more repeatable etches. For this, an accurate, repeatable measurement of [Cl] is essential.

In general, the evaluation of which sensor systems are needed or can be successful in advanced equipment control is a critical issue. Since chlorine is a very common etchant gas, this provides further motivation for evaluating methods for estimating [Cl].

Electronics Manufacturing and Control Systems Laboratory, Electrical Engineering and Computer Science Department, University of Michigan, Ann Arbor, MI 48109-2122.

Various methods for measuring [Cl] are described in the literature. Gas phase titration can be used to measure the atomic chlorine concentration downstream from the plasma [7], but the atomic chlorine concentration here may be significantly different than that in the plasma because of recombination. Laser absorption of Cl_2 has been used to measure the molecular chlorine concentration [18]; if the rest of the gas is assumed to be atomic chlorine, [Cl] can be determined. However, this technique is subject to significant errors if the atomic concentration is low, if the gas temperature is unknown, or if unknown concentrations of other species, such as etch products, are mixed with the gas. The laser must also be passed through the plasma many times using mirrors, and alignment of such systems can be difficult. Far infrared tunable diode laser absorption has been used to measure both gas temperature and [Cl] [23], but, again, the laser must be passed through the plasma many times. Two-photon laser-induced fluorescence (LIF) has also been used to measure [Cl], but the signal-to-noise ratio is poor at low pressures [15]. In addition, a very bright, high pulse frequency laser is needed for this technique, and such equipment can be prohibitively expensive. In general, for etch applications at least, laser based measurement techniques are not ready for use in a manufacturing environment.

The remainder of the paper is structured as follows. Section II reviews the fundamentals of standard actinometry and then examines the particularities of actinometry for chlorine plasmas, namely the additional pathway of excitation via dissociative excitation. The effects of dissociative excitation on the ability to estimate [Cl] via standard actinometry are analyzed in Section III, with the main result being the relationship between plasma density and relative error in the [Cl] estimate. The consequences of using this potentially inaccurate estimate as a basis to control [Cl] are analyzed in Section IV; the main result quantifies the relative error in [Cl] as a function of standard process disturbances and the relative importance of the dissociative excitation pathway. Section V shows how this error may be significantly reduced by using techniques from control theory, namely asymptotic observers, to form an improved [Cl] estimate.

II. Background Material on Optical Emission Spectroscopy

One common, non-intrusive, *in situ* measurement technique is optical emission spectroscopy (OES). With this technique, the intensity of an emission line from the species of interest is monitored. When an electron with sufficient energy hits a particle and causes one of its electrons to jump into a higher

shell, the particle is said to be excited. When the particle relaxes and the electron jumps to a lower energy state, a photon with a certain characteristic wavelength is emitted, causing the plasma to glow. The wavelength of the emitted light is determined by the difference between the excited and final energy states of the particle. Each atomic or molecular species has certain allowed energy states, resulting in a unique emission spectrum for each species [24]. The excited state of element X is denoted X^*.

The intensity at a particular wavelength is related to the concentration of the species in the plasma and other plasma properties. Specifically,

$$I_{\mathrm{X}} \propto k_{\mathrm{X}}[e^-][\mathrm{X}], \tag{1}$$

where I is the intensity, $[e^-]$ is the concentration of free electrons in the plasma, [X] is the concentration of species X, and k_{X} is given by

$$k_{\mathrm{X}} = \int_0^\infty v(\epsilon)\sigma_{\mathrm{X}}(\epsilon)f(\epsilon)d\epsilon, \tag{2}$$

where ϵ is the electron energy, $v(\epsilon)$ is the electron velocity, $\sigma_{\mathrm{X}}(\epsilon)$ is the collision cross section for excitation of species X at the monitored wavelength, and $f(\epsilon)$ is the electron energy distribution function [17]. Notice that emission intensity is a function of electron energy and concentration, so that increasing the number of high energy electrons will cause a brighter glow even if the species concentration remains the same.

A. Standard actinometry

To correct for the effects of electron concentration and energy, Coburn and Chen introduced the concept of actinometry in 1980 [5]. In actinometry, a small amount of inert gas is introduced into the plasma, and the ratio of the emission intensities of the species of interest and the inert species is monitored. Letting Act denote the actinometer, the fundamental relation of actinometry is:

$$\frac{I_{\mathrm{X}}}{I_{\mathrm{Act}}} \propto \frac{k_{\mathrm{X}}}{k_{\mathrm{Act}}}\frac{[\mathrm{X}]}{[\mathrm{Act}]}. \tag{3}$$

If the collision cross sections of the two excitation reactions are similar functions of electron energy or if the electron energy distribution remains constant, $k_{\mathrm{X}}/k_{\mathrm{Act}}$ can be regarded as a constant. It has been shown that the similarity of shapes of the collision cross sections is not as important as the similarity of excitation thresholds [3, 19].

From (3), if [Act] is measurable, say by mass spectrometry[1] [14], then

$$[\mathrm{X}] \propto \frac{\mathrm{I_X}}{\mathrm{I_{Act}}}[\mathrm{Act}].$$

Alternatively, if the amount of dissociation of the feed gas is small and the flow of the inert gas is a constant percentage of the total flow, then [Act] will be approximately proportional to the pressure, P, [13, 16] resulting in

$$[\mathrm{X}] \propto \mathrm{P}\frac{\mathrm{I_X}}{\mathrm{I_{Act}}}.$$

As with all measurement techniques, actinometry is based on some assumptions. The assumption that the collision cross sections are similar functions of electron energy was already recalled. One necessary condition for this is that the two emission reactions have similar threshold energies. Another important assumption is that the excited state resulting in emission at the wavelength being monitored occurs only via electron impact excitation of the ground state,

$$e^- + \mathrm{X} \rightarrow \mathrm{e}^- + \mathrm{X}^*.$$

This assumption is true for both the 750 nm and 811.5 nm Ar emission lines [12], for example. Furthermore, a constant fraction of the excited species must relax by photon emission.

Note that actinometry does not result in an absolute measurement of the species concentration because the components of the proportionality constant are not well known. The measurement is thus in arbitrary units (i.e., un-scaled), but this will not pose a problem for feedback control of [Cl] as long as the gain of the OES system is time-invariant (i.e., the sensor gain remains constant over time).

B. Actinometry to measure atomic chlorine concentration

Actinometry has been shown to work well for measuring [F] [5, 11], but there is considerable dispute as to its validity for measuring Cl in Cl_2 plasmas [1, 6, 11, 17]. Gottscho and Donnelly studied linewidths of the Cl 837.6 nm and Ar 826.4 nm emission lines, because narrow lines tend to be caused by ground-state excitation, whereas dissociative excitation tends to cause wider lines due to Doppler broadening

[1] It is difficult to measure [Cl] with a mass spectrometer. First, some of the atomic chlorine in the plasma would recombine to form Cl_2 on the way to the ionizer, so the concentration of atomic chlorine at the mass spectrometer does not necessarily equal that in the plasma. Second, because the ionizer cracks and ionizes some of the species to measure the number of particles with a certain mass-to-charge ratio, some of the molecular chlorine is converted to Cl atoms. The second effect can be corrected if the cracking patterns of molecular chlorine are well known at the electron energies used [8]. Neither of these problems occurs with inert gases such as argon or xenon, however. Finally, the reaction of Cl or Cl_2 with the ionizer can cause significant changes in the calibration of the mass spectrometer.

[11]. The observed linewidths were similar in the center of the plasma but not in the sheaths, so the authors of [11] concluded that actinometry should be reliable as long as either spatially unresolved emission or emission only from the plasma center is used. However, Richards et al. used spatially unresolved emission and found that actinometry is not valid for Cl_2 plasmas [17]. Aydil and Economou [1] used spatially resolved actinometry of the 808.7 nm and 837.6 nm Cl lines and the 811.5 nm Ar line from the center of the plasma. When using the 808.7 nm Cl line, these authors saw good correlation between the dependence of Cl on pressure and power and the dependence seen in laser absorption measurements by Richards et al. [17]. The 837.6 nm Cl line did not exhibit the same dependence.

One problem with actinometry in Cl_2 plasmas is that excitation can occur by electron impact dissociation and by dissociative attachment:

$$Cl_2 + e^- \rightarrow Cl^* + Cl + e^- \tag{4}$$

$$Cl_2 + e^- \rightarrow Cl^* + Cl^-, \tag{5}$$

violating the assumption that excitation occurs only by ground-state electron impact. Examining the electron energies needed for these reactions shows that they may be quite important. The Cl–Cl bond strength is 2.5 eV, while the excitation threshold is 10.4 eV for the 837.6 nm Cl emission line [17]. Thus, an electron would need 12.9 eV of energy for the reaction in (4) to occur. When an electron attaches to Cl, 3.2 eV is released, and therefore an electron with at least $12.9 - 3.2 = 9.7$ eV of energy could cause the reaction in (5). Due to the low bond strength of Cl–Cl, the energies needed for these reactions are close to the threshold energy for ground state excitation. Using k_{de} to denote the combined rate coefficient of reactions (4) and (5), the emission intensity of Cl can be expressed as

$$I_{\mathrm{Cl}} \propto k_{\mathrm{Cl}}[e^-][\mathrm{Cl}] + \mathrm{k_{de}}[\mathrm{e^-}][\mathrm{Cl_2}]. \tag{6}$$

Notice that the intensity depends on the concentrations of both Cl and Cl_2, but it is not known what percentage of the emission from the bulk plasma is caused by each excitation mechanism as the collision cross sections and electron energy distribution function are unknown. It is possible that Aydil and Economou [1] found better results with the 808.7 nm Cl line than with the 837.6 nm line because the 808.7 nm line has a higher excitation threshold of 12.0 eV. Electrons must therefore have a higher energy to cause dissociative excitation, and there is also less difference between the Cl excitation threshold and the Ar excitation threshold. Unfortunately, there are several Cl emission lines in the

neighborhood of 808.7 nm, and they are difficult to resolve. It is the authors' experience that the emissions from these lines are very dim in comparison to the 837.6 nm line.

Donnelly [9] alleviated the dissociative excitation problem by measuring $[Cl_2]$ using actinometry and calculating [Cl] from the $[Cl_2]$ measurement. The $[Cl_2]$ measurement is done by dividing the 306 nm Cl_2 emission by the 823.2 nm xenon emission. Xenon is used as an actinometer because its excitation threshold, 9.82 eV, is closer than the argon threshold (13.47 eV) to the Cl and Cl_2 thresholds (10.4 eV at 822.2 nm and 8.4 or 9.2 eV at 306 nm, respectively)[2]. Donnelly noted that at high powers, the Cl_2 in the reactor was almost completely dissociated and therefore, if only Cl and Cl_2 are present in the reactor, a small error in the $[Cl_2]$ measurement will not significantly affect the calculation of [Cl]. In low density plasmas, however, small errors in $[Cl_2]$ measurement could lead to large errors in the calculated [Cl]. Furthermore, the emission lines used by Donnelly are over 500 nm apart. This could lead to problems as the transmission versus wavelength through windows may change due to coating by etch products and/or etching of the window.

Taking dissociative excitation into account, the equation for Cl actinometry becomes

$$\frac{I_{\mathrm{Cl}}}{I_{\mathrm{Act}}} \propto \frac{k_{\mathrm{Cl}}}{k_{\mathrm{Act}}}\left(\frac{[\mathrm{Cl}]}{[\mathrm{Act}]}\right) + \frac{k_{de}}{k_{\mathrm{Act}}}\left(\frac{[\mathrm{Cl_2}]}{[\mathrm{A_{act}}]}\right), \tag{7}$$

where Act is the actinometer. This equation can be rewritten as

$$\frac{I_{\mathrm{Cl}}}{I_{\mathrm{Act}}} = K_{act}\left(\frac{[\mathrm{Cl}]}{[\mathrm{Act}]} + \mu\frac{[\mathrm{Cl_2}]}{[\mathrm{Act}]}\right), \tag{8}$$

where K_{act} is $k_{\mathrm{Cl}}/k_{\mathrm{Act}}$ times the proportionality constant, and μ is $k_{\mathrm{de}}/k_{\mathrm{Cl}}$. When $\mu = 0$, this expression reduces to the standard actinometry equation.

III. Effects of Dissociative Excitation on [Cl] Estimation Accuracy

Since the magnitude of the dissociative excitation component of the chlorine optical emission signal is unknown, it is tempting to ignore it and to apply the standard actinometry formula for estimating [Cl], that is, to assume that $\mu = 0$. This section determines the accuracy of the standard actinometric [Cl] estimate as a function of μ and the dissociation fraction of Cl_2 in the plasma. In this analysis, it is assumed that Act is a perfect actinometer and that its concentration is known. In practice, Act would probably be either Ar or Xe.

[2]Although Xe is a more appropriate actinometer for chlorine than Ar, xenon is not currently available on our system, so argon is used for this work. Richards et al. [17] report that argon and xenon yielded similar results in chlorine actinometry studies.

Represent the measured intensity ratio as

$$I_{rat} = K_{act}\left(\frac{[\mathrm{Cl}]}{[\mathrm{Act}]} + \mu\frac{[\mathrm{Cl_2}]}{[\mathrm{Act}]}\right), \tag{9}$$

and define the dissociation fraction, D, by

$$D = \frac{[\mathrm{Cl}]/2}{[\mathrm{Cl}]/2 + [\mathrm{Cl_2}]}. \tag{10}$$

Solving for $[\mathrm{Cl_2}]$ in (10), and substituting into (9) yields

$$I_{rat} = K_{act}\frac{[\mathrm{Cl}]}{[\mathrm{Act}]}\{1 + \frac{\mu(1-D)}{2D}\}. \tag{11}$$

Assume now that $\mu = 0$, and solve for [Cl] in (9) to obtain the standard actinometric estimate:

$$[\mathrm{Cl}]_{\mathrm{Act}} = \frac{\mathrm{I_{rat}}}{\mathrm{K_{Act}}}[\mathrm{Act}], \tag{12}$$

whereas, for $\mu \neq 0$, the true value of [Cl] is actually

$$[\mathrm{Cl}]_{\mathrm{true}} = \frac{\mathrm{I_{rat}}}{\mathrm{K_{Act}}}[\mathrm{Act}]\frac{1}{1 + \frac{\mu(1-\mathrm{D})}{2\mathrm{D}}}. \tag{13}$$

A little algebra yields the percent relative chlorine estimation error as a function of μ and D:

$$\frac{[Cl]_{Act} - [Cl]_{true}}{[Cl]_{true}} \times 100\% = \frac{\mu(1-D)}{2D} \times 100\%. \tag{14}$$

Note that the relative error of the standard actinometric [Cl] estimate is directly proportional to relative intensity of the optical emission line coming from dissociative excitation (i.e., μ), and that it is quite sensitive to the fraction of $\mathrm{Cl_2}$ that is dissociated in the plasma. Figure 1 depicts the relative error in the standard actinometric [Cl] estimate when $\mu = 0.1$. Other values are easily obtained by scaling. For example, if $\mu = 0.2$, the relative error in the chlorine estimate exceeds 10% for $0 < D < 0.5$. Hence, for a wide range of plasma conditions, and especially under low density conditions, the error in the standard actinometric estimate of [Cl] may be too large for it to be very useful for monitoring or regulating [Cl]. This is investigated in the next section.

IV. Effects of Dissociative Excitation-Induced Measurement Error on Feedback Control

This section assesses the effects of the dissociative excitation-induced measurement error on the use of the OES signal for feedback control of [Cl]. A simple dynamic model of a chlorine plasma in an RIE

is used to determine the range of μ for which adjusting the power applied to the plasma in order to maintain the standard actinometric estimate of [Cl] constant in the face of typical plasma perturbations results in better regulation of [Cl] than a standard practice control policy, where the power is kept constant. The plasma perturbations considered include mass flow controller drifts, pressure sensor error, power setpoint drift (due to imperfect matching, for example), and loading.

A. Simplified plasma model

The following continuously-stirred tank reactor model is used to assess the relative merits of various control strategies. The model represents average concentrations of species in the bulk plasma and mainly captures the dissociation of Cl_2 and the resulting dilution of the actinometer.

$$[\dot{Act}] = \frac{Act_{in}}{V} - \frac{L}{V}\frac{[Act]}{[Act]+[Cl_2]+[Cl]} \tag{15}$$

$$[\dot{Cl}_2] = \frac{Cl_{2in}}{V} - \frac{L}{V}\frac{[Cl_2]}{[Act]+[Cl_2]+[Cl]} - k[e][Cl_2] \tag{16}$$

$$[\dot{Cl}] = 2k[e][Cl_2] - \frac{L}{V}\frac{[Cl]}{[Act]+[Cl_2]+[Cl]}. \tag{17}$$

In the above, $[\dot{X}] = \frac{d}{dt}[X]$, Act_{in} and Cl_{2in} are the flows of Act and Cl_2 gas, respectively, V is the chamber volume, L is a loss factor which represents gases being pumped out through the throttle or lost to the walls, and $k[e]$ is the rate constant of dissociation (with or without excitation) times the concentration of electrons. The term $k[e]$ is used in the model as an input similar to power. All species are assumed to stick to the walls equally, and hence the state of the walls is not taken into account, being effectively absorbed into the loss term. The effect of [Cl] on [e^-] is not modeled, although chlorine atoms will scavenge some electrons. Pressure is calculated using the ideal gas law,

$$P = \frac{nRT}{V} = ([Act]+[Cl_2]+[Cl])RT, \tag{18}$$

with T taken as room temperature. Inputs to the model are Act flow, Cl_2 flow, $k[e]$, and loss (or pumping) rate, L. Outputs are [Act], [Cl_2], [Cl], pressure (18), dissociation fraction (10) and intensity ratio, calculated by

$$I_{rat} = \frac{[\mathrm{Cl}]}{[\mathrm{Act}]} + \mu\frac{[\mathrm{Cl}_2]}{[\mathrm{Act}]}, \tag{19}$$

where, for convenience, K_{Act} has been normalized to one.

B. Effect of μ on feedback control of [Cl]

For the model (15-17), standard PID controllers can be designed as shown in Figure 2 to regulate pressure, P, and the *estimated* chlorine concentration, $[\mathrm{Cl}]_{est}$, to desired values, P^* and [Cl]*, respectively, with zero steady state error. For the purposes of this analysis, the chlorine estimate will be formed in two ways. The first assumes that the actinometer concentration can be measured on line, say by mass spectrometry, [14],

$$[Cl]_{Act} := I_{rat}[Act]. \tag{20}$$

The second estimate assumes that [Act] is not directly measurable and must be approximated by $\alpha \times P$, where α is the fraction of the actinometer metered in the feedgas ($\frac{Act_{in}}{Act_{in}+Cl_{2in}}$); this yields [13, 16]

$$[Cl]_P := \alpha I_{rat} P. \tag{21}$$

The nominal steady-state species concentrations for given gas flows, P^*, and desired dissociation fraction, D^*, can be calculated by setting the derivatives in (15-17) to zero and using (18) and (10) to solve for [Act],[C l], and [Cl_2]. The nominal values of k[e] and L can also be found. The nominal chlorine estimates can be calculated for various values of μ using (20) and (21).

The steady-state species concentrations using *standard practice* control, where pressure and "power" are held constant, are determined by using (15-17) along with (18) and the value of k[e] found in the nominal case. Loading is introduced by multiplying the L in (17) by β, where β is the loading. For example, $\beta = 1.1$ would designate a load of 1.1 times the nominal value, or a 10% increase in loading of atomic chlorine.

The steady-state species concentrations using actinometry to control [Cl] were found by using (15-17) and (18). The final necessary equation in each scenario is formed by setting the chlorine estimate using the actinometric feedback-based values of species concentrations (and pressure, when [Act] cannot be measured) equal to the appropriate estimate calculated for the nominal case for each μ. The relative error can be found using (14) with the feedback-based and nominal values of [Cl]. Doing so yields, for actinometry using an [Act] measurement, (20):

$$\text{rel [Cl] error} \quad = \quad \left(\frac{Act_{in}\left[\frac{E_1}{E_3}(2D + \mu(1-D)) - \mu E_0 E_2 - D E_1(2 - \mu\beta)\right]}{Act_{in} E_1 D(2-\mu\beta) + 2Cl_{2in} E_2 D(1-\mu)} \right.$$

$$+\frac{Cl_{2in}\left[\frac{E_2}{E_3}(2D+\mu(1-D))-\mu E_0 E_2(1+D)-2DE_2(1-\mu)\right]}{Act_{in}E_1D(2-\mu\beta)+2Cl_{2in}E_2D(1-\mu)}\Bigg)\times 100\%, \quad (22)$$

where

$$\begin{aligned} E_0 &= 1 + \text{relative error in pressure} \\ E_1 &= 1 + \text{relative error in Act flow} \\ E_2 &= 1 + \text{relative error in } Cl_2 \text{ flow} \\ E_3 &= 1 + \text{relative error in [Act] measurement} \\ \beta &= 1 + \text{relative loading effect.} \end{aligned} \quad (23)$$

For actinometry using a pressure measurement, (21), the relative error is

$$\text{rel [Cl] error} = \left(\frac{E_0}{\beta D Act_{in}}\frac{[Act_{in}+Cl_{2in}(1+D)]\left[\left(\frac{E_2}{E_1}-1\right)\mu+D(\mu-2)\right]}{\mu-\frac{2}{\beta}+\frac{Cl_{2in}}{Act_{in}}\left[(1-\frac{2}{\beta})(2D+\mu(1-D))+\frac{2}{\beta}(\mu-1)\frac{E_2}{E_1}\right]}-1\right)\times 100\%, \quad (24)$$

where E_0, E_1, E_2, and β are defined as above. It should be mentioned that in this case the pressure used in the chlorine estimate is the *measured* pressure, which will not necessarily be equal to the chamber pressure, due to E_0. In this analysis, the measured pressure is taken to be equal to the nominal pressure setpoint. This is because pressure is held constant through feedback control, and if there is a pressure sensor error, the chamber pressure will be incorrect but the pressure sensor will give the nominal reading.

Note that in both cases, the pressure error affects the relative [Cl] error, but the pressure itself does not.

Tables I and II compare the effectiveness of the feedback controllers to the standard practice scheme. The comparison is in terms of maintaining a constant chlorine concentration in the face of common process and equipment perturbations for μ ranging from zero to one and for D equal to 0.1 or 0.7. The values in the tables are percent relative chlorine concentration errors with respect to the nominal process conditions established under no perturbations. For example, in Table I, the nominal process conditions are 10 sccm Cl_2, 1 sccm Act, 5 mTorr pressure, and k[e] adjusted to yield a "high density" plasma having 70% of the Cl_2 dissociated. This corresponds to [Cl]= $1.3 \times 10^{14}/cm^3$. The nominal conditions were then disturbed by introducing the following perturbations, one by one: reducing the Cl_2 flow rate by 10%; increasing the pressure by 10 /to simulate a pressure reading that was 10%

low; reducing delivered "power" by 10%; and finally, increasing the loss rate of Cl in (17) by 10 % to represent loading caused by seasoning or etching.

The relative errors in the case of standard practice control do not depend on μ because μ affects only the intensity ratio measurement, which is not used in this case. When $\mu = 0$, as in standard actinometry, the $[Cl]_{Act}$-based controller perfectly rejects all tested disturbances and maintains [Cl] at the desired level. For example, when the actual chlorine flow is lower than nominal, which represents an error in the mass flow controller, the residence time of the Cl_2 is increased, and hence more of it is dissociated. The controller therefore decreases $k[e]$ to decrease the [Cl]. When $\mu > 0$ and the accuracy of the estimate $[Cl]_{Act}$ degrades, more of the signal is coming from dissociative excitation of the Cl_2. Because of the increase in [Cl], $[Cl_2]$ is decreasing, and therefore the intensity ratio does not rise as much as it would if $\mu = 0$. The controller therefore does not see as much increase in [Cl] and does not lower $k[e]$ enough to compensate. The result is an increased steady-state [Cl] concentration.

The controller based on $[Cl]_P$ is seen to be very sensitive to flow errors in Cl_2, and though not shown in the tables, it has a similar sensitivity to flow errors in the actinometer. This is due to the resulting change in the proportion [Act]/P. This sensitivity can be greatly reduced by using a feedgas that is pre-mixed with a fixed percentage[3] of the actinometer. When this is done a 10% drop in total flow rate results in less than 0.1% errors, for μ between zero and one for both of the process conditions considered here. The performance of the $[Cl]_{Act}$-based controller with a 10% drop in total flow improves as well to near perfect regulation of [Cl] for the entire range of μ considered.

The standard practice and $[Cl]_P$-based controllers are very sensitive to errors in the pressure measurement. This sensitivity is also apparent in the $[Cl]_{Act}$-based controller, except when μ is very small. We can see that as μ increases, the $[Cl]_{Act}$-based controller causes even greater errors in [Cl] than the standard practice controller. Indeed, for many of the perturbations studied, the error in [Cl] using standard actinometry increases past the error using standard practice control as μ increases.

In summary, these results show that for small μ, closed-loop control using standard actinometry can be quite beneficial. However, as μ increases and the assumptions behind standard actinometry become increasingly incorrect, using actinometry for feedback can cause greater errors in [Cl] than those seen in the standard practice case, despite the fact that the actinometric trend with power and pressure is

[3]If a more complicated chemistry is used, the actinometer should be pre-mixed to a fixed percentage in all of the gases

correct. It is thus necessary to more closely determine μ before attempting to control [Cl] using optical measurements.

V. Improved [Cl] Estimation for Larger μ

Section IV showed that as long as the contribution of the dissociative excitation to the chlorine emission line is sufficiently small, the standard actinometric formula for chlorine estimation could be used to advantage in a feedback control loop. However, when the dissociative excitation contribution becomes larger, say for $\mu > 0.3$, the errors in the resulting estimate of the chlorine concentration lead to the control loop's performance being no better, on even worse, than that of a standard practice control policy. This section addresses how to obtain an improved estimate of bulk chlorine concentration if μ and K_{act} are known.

For the simplified chemical model (15-17), if I_{rat}, P and [Act] are each measurable, then, as long as $\mu \neq 1$, it is possible to directly solve for the chlorine concentration in terms of μ, denoted $[\mathrm{Cl}]_\mu$, to obtain

$$[Cl]_\mu = \frac{1}{1-\mu}\left\{\frac{I_{rat}}{K_{act}}[Act] - \mu(\frac{P}{RT} - [Act])\right\}. \tag{25}$$

Then, to the extent that the parameters and measurements appearing in the above equation are available and sufficiently accurate, $[\mathrm{Cl}]_\mu$ could be used as the basis of a feedback control policy.

On the other hand, if the chemistry contains additional species, such as HBr, O_2 or etch products, or if [Act] cannot be directly measured, then one is no longer in the situation of three equations and three unknowns, and other means must be used to recover an estimate of the chlorine concentration. One such method, based on asymptotic observers [2, 20], is studied in the next subsection.

A. Observers

Consider again the situation of the simplified chemical model (15-17), and assume that I_{rat} and P are measurable, but that [Act] is not. Write the model as

$$\dot{x} = f(x,u) \tag{26}$$

$$y = h(x), \tag{27}$$

where the model's states, inputs and outputs are respectively,

$$x = \begin{bmatrix} [Act] \\ [Cl_2] \\ [Cl] \end{bmatrix}, u = \begin{bmatrix} Act_{in} \\ Cl_{2in} \\ L \\ k[e] \end{bmatrix}, y = \begin{bmatrix} P \\ I_{rat} \end{bmatrix}.$$

A well-known means from the control literature of recovering estimates, $\hat{x}$, of the states of a model from the available measurements, y, is to use an asymptotic observer:

$$\begin{aligned} \dot{\hat{x}} &= f(\hat{x}, u) + L(y - \hat{y}) \\ \hat{y} &= h(\hat{x}), \end{aligned} \tag{28}$$

where L, the observer gain, is to be chosen so that $lim_{t\to\infty}(\hat{x}(t) - x(t)) = 0$, at least if the initial state of the estimator is not too far off from the state of the model. If the model is augmented with a description of noise statistics for the outputs and states, and L is selected to minimize the covariance of the estimate, then (28) is called a constant coefficient extended Kalman filter (EKF). In this study, L will be a 3×2 matrix of constants selected to (locally, exponentially) stabilize the estimator. This is possible if, and only if, the linearization of the system (26) about a nominal operating point is detectable. A very important sufficient condition for this to hold is that the linearization be *observable* [4], which means that for any given input, distinct state trajectories give rise to distinct output trajectories (measurement histories). This condition will be analyzed in the next two subsections.

B. Observability analysis

This subsection first briefly recalls some basic facts on how to the check the observability condition discussed above [2, 20]. This condition is then applied to the model in order to understand when it is possible to recover [Cl] from the available measurements.

Denote the linearized model at a given operating point u_{nom}, x_{nom} by

$$\dot{x} = Ax + Bu \tag{29}$$

$$y = Cx \tag{30}$$

where, $A = \frac{\partial f(x_{nom}, u_{nom})}{\partial x}$, $B = \frac{\partial f(x_{nom}, u_{nom})}{\partial u}$, and $C = \frac{\partial h(x_{nom})}{\partial x}$. According to standard control theory,

a system is observable when the observability matrix, $\mathcal{O}$, is full rank, where

$$\mathcal{O} = \begin{bmatrix} C \\ CA \\ \vdots \\ CA^{n-1} \end{bmatrix}, \tag{31}$$

and n is the number of states (for the model under consideration, $n = 3$). In practice, it is useful to look at the singular value decomposition (SVD) of $\mathcal{O}$ to determine its numerical rank. The SVD finds unitary matrices U and V to solve the equation

$$\mathcal{O} = USV^T$$

where S is a matrix with the singular values on the main diagonal and zeros elsewhere. If the singular values are all non-zero and roughly the same magnitude, the observability matrix is full-rank. If there are large differences between the singular values, or more specifically, if the condition number[4] is large, the matrix is numerically almost rank-deficient, meaning that the given set of measurement equations does not contain adequate information to estimate all of the states of the model. The almost unobservable state or states correspond to the approximate (or numerical) nullspace of $\mathcal{O}$. In any observer design, unobservable states simply evolve according to the system's dynamics (26), and are unaffected by the output injection term, $L(y - \hat{y})$ in (28); these states are thus not corrected by the measurements. A final point is that an SVD is not scale independent. It is important to scale the measurements appropriately to the problem at hand. In this analysis, the magnitude of I_{rat} will be scaled to equal that of P at each operating point that is analyzed. The states are scaled so that the nominal value of each component is one.

The condition number of the observability matrix of the linearized model is displayed in Table III for a wide range of μ and D. The process conditions are 20 mTorr pressure and a flow of 20 sccm 95%/5% Cl_2/Act. A condition number on the order of ten or less indicates a qualitatively well-observable system and thus a system for which an observer may be successfully designed. The table shows that the model is well observable for all ranges of μ considered when $0.3 \leq D \leq 0.7$, and for a restricted range of μ when $D = 0.2$ or 0.8. Further analysis not shown here indicates that when $D = 0.8$, the loss of observability is mainly attributable to [Cl_2], and not to [Cl] nor [Act].

[4]The condition number is the ratio of the largest to the smallest singular value.

C. Typical observer performance

Following standard methods in control theory, the observer (28) was designed and incorporated into a feedback controller as show in in Figure 3. The steady-state performance of the observer-based feedback controller was then examined. Table IV displays the percent relative error in [Cl] (with respect to nominal) under the same process perturbations considered previously: reducing the Cl_2 flow rate by 10%; pressure sensor providing a reading that was 10% low; reducing delivered "power" by 10%; and finally, to represent loading caused by seasoning or etching, the loss rate of Cl in (17) was increased by 10%. The setpoint for the observer-based controller was determined in the following manner. Once the nominal process conditions were set up, namely flow, pressure and dissociation fraction, the corresponding value of $[Cl]_{est}$ from the observer was determined and used as the setpoint for the closed-loop controllers. In this way, under nominal conditions, the desired process conditions are maintained in all cases. The performance of the controllers was then evaluated, as explained above, for various disturbances.

Table V evaluates the robustness of the observer. The above numerical simulations were repeated with the same observer applied to an imperfect model. The perturbed model had power reduced by 10% and Cl_2 flow increased by 5%. The performance of the closed-loop system is still greatly improved over the situation analyzed in Section IV.

VI. Conclusions

For advanced process control, it is vitally important to know which sensor systems are needed or can be successful. Whenever possible, an error analysis should be performed prior to the implementation of any sensor system.

An analysis of a simplified plasma model has shown that when using actinometry to measure and control [Cl], it is essential to know how much of the emission is coming from dissociative excitation. If control is applied using standard actinometry, the closed-loop response to disturbances can be worse than the corresponding response under standard-practice open-loop control, for sufficiently large μ. However, as μ approaches zero, standard actinometry becomes valid, and the closed-loop performance shows improvement over the standard practice results. If μ is large, and known, then techniques from control theory, namely asymptotic observers, may be used to estimate the chlorine concentration, and

this estimate can be used to advantage in a feedback loop.

Acknowledgments

This work was supported in part by AFOSR/DARPA under MURI Grant No. F49620-95-1-0524 and the SRC under contract number 97-FC-085.

References

[1] E. S. Aydil and D. J. Economou, "Theoretical and experimental investigations of chlorine RF glow discharges, II. Experimental," *Journal of the Electrochemical Society*, vol. 139, no. 5, pp. 1406–1412, May 1992.

[2] W. Bauman and W. J. Rugh, "Feedback control of nonlinear systems by extended linearization," *IEEE Transactions on Automatic Control*, vol. 31, no. 1, pp. 40–46, 1986.

[3] J. P. Booth, O. Joubert, J. Pelletier, and N. Sadeghi, "Oxygen atom actinometry reinvestigated: Comparison with absolute measurements by resonance absorption at 130 nm," *Journal of Applied Physics*, vol. 69, no. 2, pp. 618–626, January 1991.

[4] C.-T. Chen, *Linear System Theory and Design*, Saunders College Publishing, 1984.

[5] J. W. Coburn and M. Chen, "Optical emission spectroscopy of reactive plasmas: A method for correlating emission intensities to reactive particle density," *Journal of Applied Physics*, vol. 51, no. 6, pp. 3134–3136, June 1980.

[6] R. d'Agostino, F. Cramarossa, S. De Benedictis, and F. Fracassi, "Optical emission spectroscopy and actinometry in CCl_4–Cl_2 radiofrequency discharges," *Plasma Chemistry and Plasma Processing*, vol. 4, no. 3, pp. 163–178, 1984.

[7] D. A. Danner and D. W. Hess, "Reaction of atomic and molecular chlorine with aluminum," *Journal of Applied Physics*, vol. 59, no. 3, pp. 940–947, February 1986.

[8] V. M. Donnelly, "Mass spectrometric measurements of neutral reactant and product densities during Si etching in a high-density helical resonator Cl_2 plasma," *Journal of Applied Physics*, vol. 79, no. 12, pp. 9353–9360, June 1996.

[9] V. M. Donnelly, "Optical and mass spectrometric diagnostic methods for plasma etching," in *Materials Research Society Symposium Proceedings*, volume 406, pp. 3–13. Materials Research Society, 1996.

[10] V. M. Donnelly, D. L. Flamm, W. C. Dautremont-Smith, and D. J. Werder, "Anistropic etching of sio2 in low-frequency cf4/o2 and nf3/ar plasmas," *Journal of Applied Physics*, vol. 55, no. 1, pp. 242–252, January 1984.

[11] R. A. Gottscho and V. M. Donnelly, "Optical emission actinometry and spectral line shapes in rf glow discharges," *Journal of Applied Physics*, vol. 2, pp. 245–250, July 1984.

[12] A. Granier, D. Chéreau, K. Henda, R. Safari, and P. Leprince, "Validity of actinometry to monitor oxygen atom concentration in microwave discharges created by surface wave in O_2-N_2 mixtures," *Journal of Applied Physics*, vol. 75, no. 1, pp. 104–114, January 1994.

[13] P. D. Hanish, J. W. Grizzle, M. D. Giles, and F. L. Terry, Jr., "A model-based technique for real-time estimation of absolute fluorine concentration in a CF_4/Ar plasma," *Journal of Vacuum Science and Technology A*, vol. 13, no. 3, pp. 1802–1807, May/June 1995.

[14] J. Jenq, J. Ding, J. W. Taylor, and N. Hershkowitz, "Absolute fluorine atom concentrations in RIE and ECR CF_4 plasmas measured by actinometry," *Plasma Sources Science Technology*, vol. 3, pp. 154–161, 1994.

[15] K. Ono, M. T. amd Kazuyasu Nishikawa, T. Oomori, and K. Namba, "Chemical kinetics of chlorine in electron cyclotron resonance plasma etching of Si," *Japanese Journal of Applied Physics Part 1*, vol. 33, no. 7B, pp. 4424–4432, 1994.

[16] B. A. Rashap, M. Elta, H. Etemad, J. P. Fournier, J. S. Freudenberg, M. D. Giles, J. W. Grizzle, P. T. Kabamba, P. P. Khargonekar, S. Lafortune, J. R. Moyne, D. Teneketzis, and F. L. Terry, Jr., "Control of semiconductor manufacturing equipment: Real-time feedback control of a reactive ion etcher," *IEEE Trans. Semi. Man.*, vol. 8, no. 3, pp. 286–297, August 1995.

[17] A. D. Richards, B. E. Thompson, K. D. Allen, and H. H. Sawin, "Atomic chlorine concentration measurements in a plasma etching reactor. I. A comparison of infrared absorption and optical emission actinometry," *Journal of Applied Physics*, vol. 62, no. 3, pp. 792–798, August 1987.

[18] G. L. Rogoff, J. M. Kramer, and R. B. Piejak, "A model for the bulk plasma in an RF chlorine discharge," *IEEE Transactions on Plasma Science*, vol. 14, no. 2, pp. 103–111, April 1986.

[19] H.-J. Tiller, D. Berg, and R. Mohr, "Decomposition of CCl_4 in an rf discharge—a gas chromatography and time-resolved emission spectroscopy study," *Plasma Chemistry and Plasma Processing*, vol. 1, no. 3, pp. 247–260, 1981.

[20] B. L. Walcott, M. J. Corless, and S. H. Zak, "Comparative study of nonlinear state-observation techniques," *Int. J. Control*, vol. 45, no. 6, pp. 2109–2132, 1987.

[21] H. F. Winters and J. W. Coburn, "Surface science aspects of etching reactions," *Surface Science Reports*, vol. 14, pp. 161–269, 1992.

[22] S. Wolf and R. N. Tauber, *Silicon Processing for the VLSI Era; Volume 1—Process Technology*, chapter 18, Lattice Press, 1986.

[23] J. Wormhoudt, A. C. Stanton, A. D. Richards, and H. H. Sawin, "Atomic chlorine concentration and gas temperature measurements in a plasma etching reactor," *Journal of Applied Physics*, vol. 1, no. 1, pp. 142–148, January 1987.

[24] A. N. Zaidel', V. K. Prokof'ev, S. M. Raiskii, V. A. Slavnyi, and E. Y. Schreider, *Tables of Spectral Lines*, IFI/Plenum, 1970.

[25] G. C. H. Zau and H. H. Sawin, "Effects of O_2 Feed Gas Impurity on Cl_2 Based Plasma Etching of Polysilicon," *Journal of the Electrochemical Society*, vol. 139, no. 1, pp. 250–256, January 1992.

VII. Figures and Tables

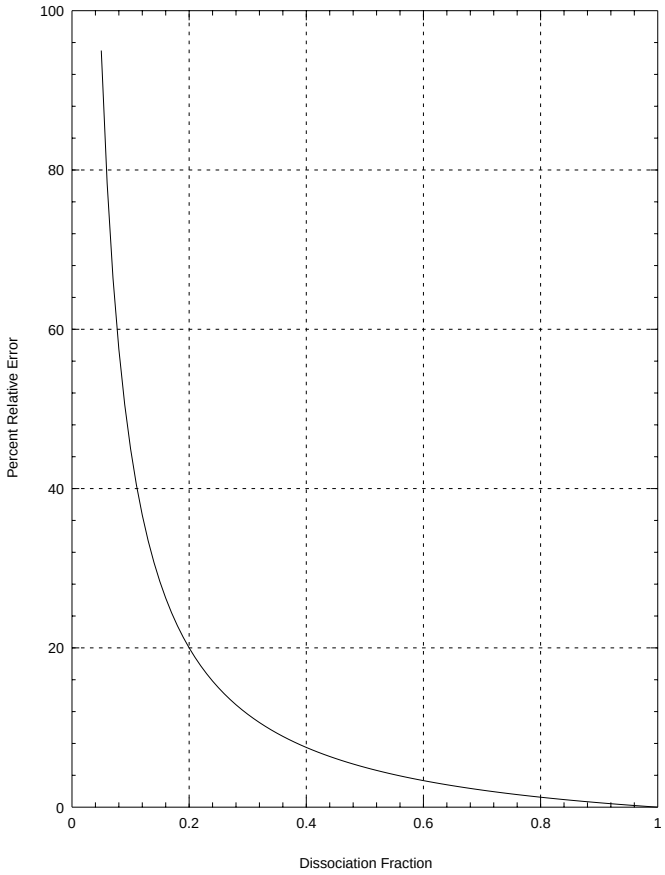

Fig. 1. Percent relative error in [Cl] estimate for μ=0.1.

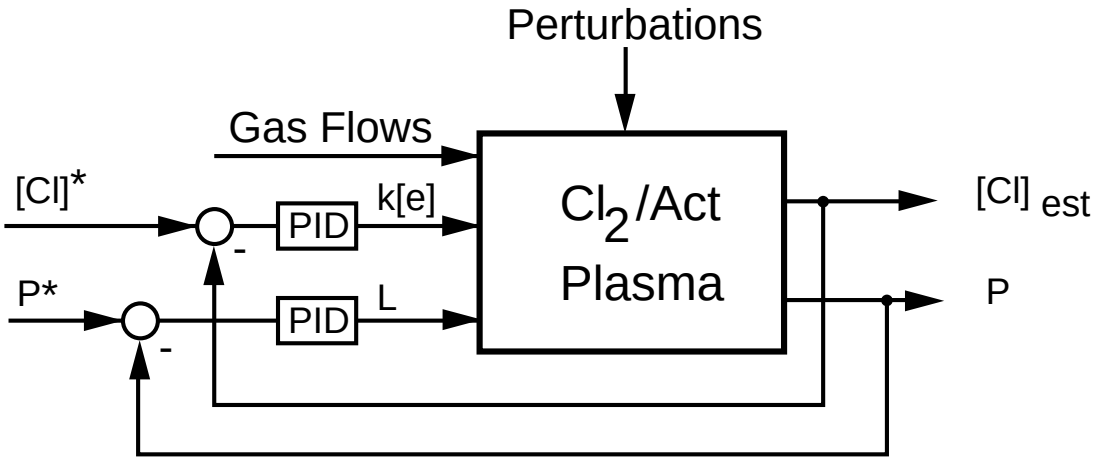

Fig. 2. Feedback control diagram.

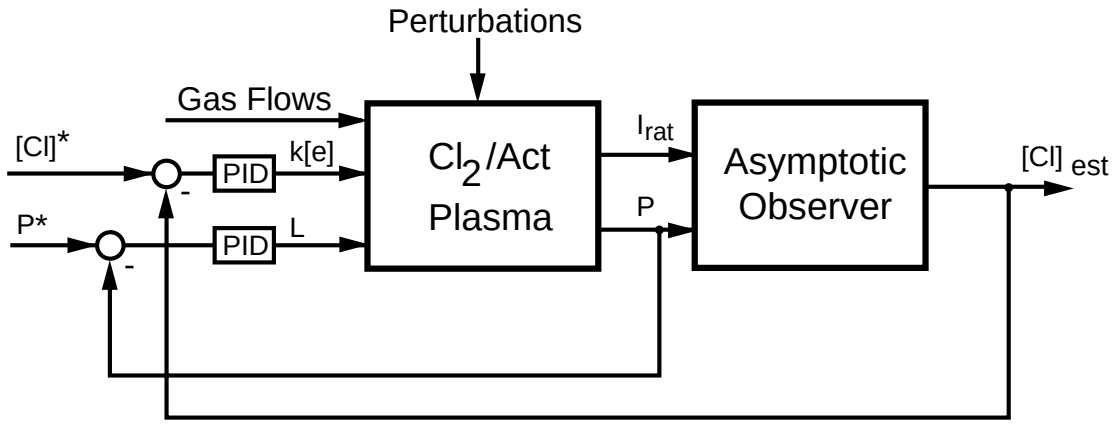

Fig. 3. Observer-based feedback control diagram.

TABLE I

%-RELATIVE ERROR IN CHLORINE CONCENTRATION UNDER STANDARD PRACTICE CONTROL, (SP), AND CLOSED-LOOP CONTROL USING $[Cl]_{Act}$ AND $[Cl]_P$. PROCESS CONDITIONS ARE 20 SCCM 95%/5% Cl_2/ACT, 5 MTORR, 0.7 DISSOCIATION FRACTION. THE NOMINAL CHLORINE CONCENTRATION IS $1.3 \times 10^{14}/cm^3$.

	Cl_2 flow 10% low			Pressure 10% high			$k[e]$ 10% low			Loading 10%		
μ	SP	$[Cl]_{Act}$	$[Cl]_P$	SP	$[Cl]_{Act}$	$[Cl]_P$	SP	$[Cl]_{Act}$	$[Cl]_P$	SP	$[Cl]_{Act}$	$[Cl]_P$
0.0	1.3	0.0	6.1	11.6	0.0	10.0	-1.7	0.0	0.0	-0.7	0.0	4.2
0.2	1.3	0.1	7.0	11.6	-3.0	10.0	-1.7	0.0	0.0	-0.7	0.1	4.9
0.4	1.3	0.3	8.2	11.6	-7.8	10.0	-1.7	0.0	0.0	-0.7	0.2	5.8
0.6	1.3	0.6	9.7	11.6	-17.2	10.0	-1.7	0.0	0.0	-0.7	0.4	7.0
0.8	1.3	1.4	11.6	11.6	-43.2	10.0	-1.7	0.0	0.0	-0.7	0.9	8.7
1.0	1.3	14.3	14.3	11.6	-100.0	10.0	-1.7	0.0	0.0	-0.7	11.1	11.1

TABLE II

%-RELATIVE ERROR IN CHLORINE CONCENTRATION UNDER STANDARD PRACTICE CONTROL, (SP), AND CLOSED-LOOP CONTROL USING $[Cl]_{Act}$ AND $[Cl]_P$. PROCESS CONDITIONS ARE 20 SCCM 95%/5% Cl_2/ACT, 20 MTORR, 0.1 DISSOCIATION FRACTION. THE NOMINAL CHLORINE CONCENTRATION IS $1.1 \times 10^{14}/cm^3$.

	Cl_2 flow 10% low			Pressure 10% high			$k[e]$ 10% low			Loading 10%		
μ	SP	$[Cl]_{Act}$	$[Cl]_P$	SP	$[Cl]_{Act}$	$[Cl]_P$	SP	$[Cl]_{Act}$	$[Cl]_P$	SP	$[Cl]_{Act}$	$[Cl]_P$
0.0	7.3	0.0	9.5	18.2	0.0	10.0	-7.8	0.0	0.0	-6.5	0.0	0.9
0.2	7.3	0.7	20.4	18.2	-13.6	10.0	-7.8	0.0	0.0	-6.5	0.1	1.9
0.4	7.3	1.8	33.7	18.2	-35.9	10.0	-7.8	0.0	0.0	-6.5	0.2	3.3
0.6	7.3	4.0	50.3	18.2	-79.2	10.0	-7.8	0.0	0.0	-6.5	0.4	5.0
0.8	7.3	10.0	71.6	18.2	-100.0	10.0	-7.8	0.0	0.0	-6.5	0.9	7.5
1.0	7.3	100.0	100.0	18.2	-100.0	10.0	-7.8	0.0	0.0	-6.5	11.1	11.1

TABLE III

OBSERVABILITY MATRIX CONDITION NUMBERS AS A FUNCTION OF μ AND D AT 20 SCCM 95%/5% Cl_2/ACT AND 20 MTORR.

μD	0.1	0.2	0.3	0.4	0.5	0.6	0.7	0.8	0.9
0.0	13.8	8.4	6.8	6.4	6.8	7.8	9.7	13.9	27.0
0.2	15.7	7.1	5.5	5.3	5.7	6.7	8.5	12.4	24.4
0.4	24.6	7.8	5.1	4.6	4.9	5.8	7.4	11.0	22.0
0.6	36.7	9.5	5.2	4.2	4.3	5.0	6.5	9.7	19.7
0.8	51.2	12.0	5.8	4.1	4.0	4.5	5.7	8.5	17.5
1.0	66.9	14.9	6.6	4.2	3.7	4.0	5.0	7.5	15.5
1.2	82.1	17.9	7.6	4.4	3.6	3.8	4.5	6.5	13.7
1.4	94.9	20.7	8.6	4.8	3.5	3.6	4.1	5.7	12.2
1.6	104.1	22.9	9.5	5.2	3.5	3.5	3.8	5.0	11.0
1.8	109.5	24.4	10.2	5.5	3.5	3.5	3.7	4.5	10.2
2.0	111.8	25.1	10.6	5.8	3.6	3.5	3.7	4.3	10.0

TABLE IV

%-Relative error in chlorine concentration under observer based feedback control. Process conditions are 20 sccm 95%/5% Cl_2/Act and 20 mTorr, with the dissociation fraction varied from 0.2 to 0.5 to 0.8.

	Cl_2 flow 10% low			Pressure 10% high			$k[e]$ 10% low			Loading 10%		
$\mu \backslash D$	0.2	0.5	0.8	0.2	0.5	0.8	0.2	0.5	0.8	0.2	0.5	0.8
0.0	1.9	5.0	1.7	15.6	16.3	13.1	-4.9	-0.5	-0.2	-4.0	1.1	0.6
0.2	3.6	5.3	1.7	18.1	16.7	13.1	-4.9	-0.4	-0.2	-3.9	1.3	0.7
0.4	4.7	5.6	1.8	19.8	17.0	13.1	-4.6	-0.3	-0.2	-3.5	1.5	0.7
0.6	5.4	5.7	1.8	20.7	17.2	13.1	-4.3	-0.2	-0.2	-3.1	1.6	0.7
0.8	5.8	5.9	1.8	21.4	17.3	13.1	-4.0	-0.1	-0.2	-2.8	1.7	0.7
1.0	6.1	6.0	1.8	21.8	17.5	13.2	-3.8	0.0	-0.2	-2.6	1.8	0.7

TABLE V

%-Relative error in chlorine concentration under observer-based feedback control, with an imperfect model. Process conditions are 20 sccm 95%/5% Cl_2/Act and 20 mTorr, with the dissociation fraction varied from 0.2 to 0.5 to 0.8.

	Cl_2 flow 10% low			Pressure 10% high			$k[e]$ 10% low			Loading 10%		
$\mu \backslash D$	0.2	0.5	0.8	0.2	0.5	0.8	0.2	0.5	0.8	0.2	0.5	0.8
0.0	3.9	7.4	2.6	17.8	19.1	14.0	-2.9	2.0	0.8	-2.1	3.7	1.6
0.2	6.9	7.9	2.6	21.9	19.5	14.0	-1.7	2.3	0.8	-0.7	4.0	1.6
0.4	8.9	8.2	2.6	24.4	19.9	14.1	-0.7	2.5	0.8	0.5	4.3	1.6
0.6	10.1	8.5	2.6	25.9	20.2	14.1	0.1	2.7	0.8	1.4	4.5	1.6
0.8	10.8	8.7	2.7	26.9	20.5	14.1	0.7	2.9	0.8	2.0	4.7	1.6
1.0	11.3	8.8	2.7	27.5	20.7	14.1	1.2	3.0	0.8	2.4	4.9	1.6